# Intramolecular Directional Energy Transfer Processes in Dendrimers Containing Perylene and Terrylene Chromophores†

**Gerd Schweitzer,‡ Roel Gronheid,‡ Sven Jordens,‡ Marc Lor,‡ Gino De Belder,‡ Tanja Weil,§ Erik Reuther,§ Klaus Müllen,§ and Frans C. De Schryver*,‡**

*Department of Chemistry, Katholieke Universiteit Leuven, Celestijnenlaan 200 F, 3001 Heverlee, Belgium, and Max-Planck-Institut für Polymerforschung, Ackermannweg 10, 55128 Mainz, Germany*

*Received: July 8, 2002; In Final Form: October 16, 2002*

The time-resolved fluorescence kinetics of a first and a second generation dendrimer with peryleneimide chromophores at the rim and a terrylenediimide chromophore in the core were investigated using femtosecond fluorescence upconversion and single photon timing techniques. By global analysis of an extentensive data set with $\lambda_{em}$ ranging from 540 to 780 nm, combining both techniques and comparing the kinetic results obtained previously for peryleneimide and terrylenediimide reference compounds, two independent energy transfer processes could be identified. The time constants were 4 and 25 ps for the first generation dendrimer and 22 and 68 ps for the second generation, respectively. They scale as expected for Förster energy transfer processes between chromophores at the distances present in the dendrimers. Each of these processes can possibly be related to different isomers present in the samples. Analysis of the in-the-bay area substituted terrylenediimide model compound reveals subsets of molecules showing different relaxation pathways of the terrylene core.

## Introduction

Dendrimers[1−8] consisting of a polyphenylene core and decorated with peryleneimide chromophores at the rim have been investigated by single-molecule spectroscopy[9−12] and time-resolved spectroscopy.[13−19] These dendrimers possess pentaphenylbenzene units and, as a result of the "interlocking" of twisted phenyl rings, are shape persistent. Further, by way of synthesis one can control the number of peryleneimide chromophores attached to the rim of the nanoparticles.[20−22]

In previous studies, the singlet excited-state relaxation processes in such dendrimers of different generation[16] and containing different numbers of peryleneimide chromophores at the rim[17] in different substitution patterns[23] were investigated. In these studies, various kinetic components could be determined and the effect of chromophore−chromophore interactions was investigated in detail.[10,16,23] However, these investigations focused on interactions between *identical* chromophores such as energy hopping,[24] singlet−singlet annihilation,[23] singlet-to-triplet energy transfer,[10] excited dimer emission,[15] and enhanced intersystem crossing.[9] The synthesis of compounds containing peryleneimide chromophores as donors and a different chromophore as acceptor extends these investigations toward directional energy transfer.[24] Preliminary reports on the synthesis[25] and energy transfer at the single molecule level[11] of such compounds have been published.

First and second generation dendrimers containing peryleneimide chromophores at the rim and a central terrylenediimide are in the focus of the ensemble time-resolved study reported here. To separate and attribute the various kinetic components, both the previously reported results from perylene-only dendrimers[16,23] and the data from a model compound ($T1P_0$), which was measured along with the actual donor−acceptor dendrimers, were taken into consideration.

## Experimental Section

In this study, four compounds have been investigated, the molecular structures of which are shown in Scheme 1. First, compound $T1P_0$, which does not contain any chromophores at the rim, was studied in order to investigate the influence of substitution of dendritic arms on the chromophore. An acronym of the type $XnY_m$ will be used throughout this paper, where X denotes the core type of the sample (e.g., terrylenediimide, T), $n = 0, 1, 2$ is the generation of the dendrimer attached to it, and $Y_m$ the type and number of chromophores attached to the rim of the molecules ($P_4$, e.g., denoting four peryleneimides). As donor−acceptor dendrimers, a first generation terrylenediimide core dendrimer ($T1P_4$) with four peryleneimide chromophores at the rim and a second generation analogue ($T2P_8$) containing 8 peryleneimide chromophores at the rim were studied. The synthesis of these compounds is decribed elsewhere in detail.[25]

The steady-state spectra were recorded using commercial spectrometers, the fluorescence quantum yields were determined using the reference compound cresylviolet; $\phi_f = 0.54$.[26]

**Femtosecond Upconversion Measurements.** Except for the excitation wavelength (see below), all other experimental conditions were kept constant and consistent with previous studies:[16,23] all measurements were performed at room temperature in 1 mm optical path length cuvettes under magic angle polarization conditions. All compounds were dissolved in toluene at a concentration that yielded an absorption of ca. 0.4 per mm at the wavelength 495 nm, which was used as the excitation wavelength for all compounds containg peryleneimide. The terrylenediimide-only compounds, however, were excited at 625 nm.

† Part of the special issue "George S. Hammond & Michael Kasha Festschrift".

* Corresponding author. E-mail: Frans.DeSchryver@Chem.KULeuven.ac.be.

‡ Katholieke Universiteit Leuven.

§ Max-Planck-Institut für Polymerforschung.

10.1021/jp026459s CCC: $25.00 
Published on Web 11/27/2002

**SCHEME 1: Molecular Structures of the Investigated Compounds**[a]

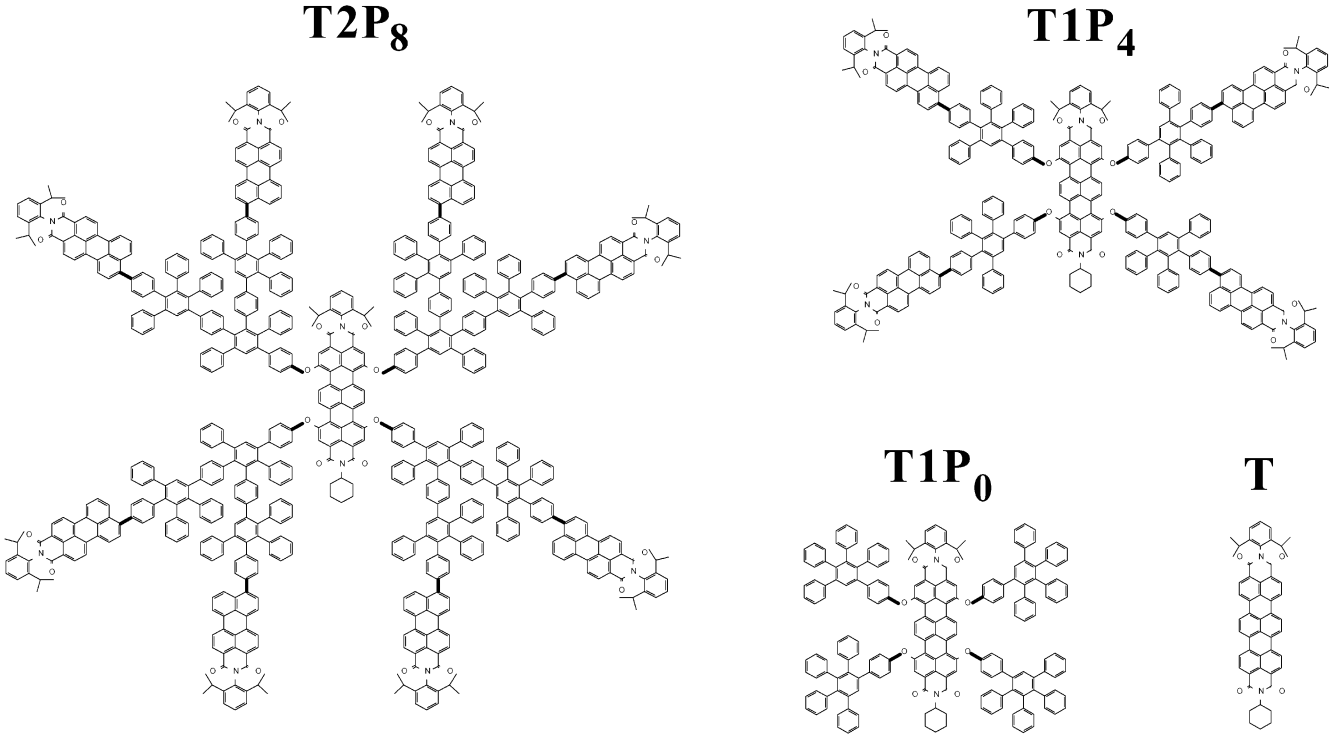


[a] T, bare chromophore; $T1P_0$, first generation model compound; $T1P_4$, first generation donor−acceptor dendrimer; $T2P_8$, second generation donor−acceptor dendrimer.

The laser system used to excite the samples has previously been described in detail.[27] In brief, a Nd:$YVO_4$ laser (Millennia V, Spectra Physics) is used to pump a Ti:sapphire laser (Tsunami, Spectra Physics). Its output seeds a regenerative amplifier (RGA, Spitfire, Spectra Physics). The output of the RGA (1 mJ, 100 fs, 800 nm) is split in two equal parts, one of which is used to pump an optical parametric generator/amplifier (OPA-800, Spectra Physics). The output wavelength range of the OPA is extended by harmonic generation using one or two BBO crystals, thus making a range of 300 nm to 900 nm accessible.

The setup used for the detection of the fluorescence upconversion signal has also been described in detail in a previous publication.[28] Briefly, the fluorescence light emitted from the sample is collected and sent to a nonlinear optical crystal, in which the sum frequency of this light and a gate pulse (800 nm, ca. 100 $\mu$J) derived from the RGA is generated. To cover a broad spectral range, two different LBO crystals were used: the first one was optimized for a low-wavelength range from 500 to 670 nm, while the second one covered the adjacent high-wavelength range from 650 to 800 nm. The time-resolved traces were then collected by detecting this sum frequency light while changing the relative delay of the gate pulse versus the sample excitation time. By detection of scattered light under otherwise typical conditions, the prompt response of this arrangement (including laser sources) was determined to be approximately 250 fs. This value was used in the analysis of all measurements for deconvolution of the data sets.

All compounds were illuminated with an excitation energy of ca. 350 nJ in an excitation spot size of 80 $\mu$m diameter. Each measurement consisted of 1024 delay positions, at each of which the fluorescence signal, the excitation laser intensity, and the gate pulse intensity were recorded averaging over five seconds, thus resulting in a measurement time ca. 5000 s per delay scan. By taking a steady-state absorption spectrum before and after each set of measurements the sample integrity under these conditions was verified.

To capture all kinetic components potentially present in the excited state dynamics as precisely as possible, a measurement as described above was then repeated using three different channel widths for the detection, resulting in total time windows of 6.7, 50, and 450 ps, respectively, for all 1024 measured channels. This set of three measurements was performed for each compound throughout its complete spectral range of interest using both nonlinear-optical crystals, thus resulting in 23 different fluorescence detection wavelengths from 530 to 750 nm at intervals of 10 nm.

**Picosecond SPT Setup.** The SPT setup, providing picosecond excitation pulses over a large part of the visible wavelength regime (360−590 nm), has been described previously.[29,30] In brief, the second harmonic of a Ti:sapphire laser (Tsunami, Spectra Physics) was used to excite the samples at 488 nm. For 590 nm excitation an optical parametric oscillator was implemented before the second harmonic generator. The fluorescence was detected under magic angle conditions (unless noted otherwise) using a double monochromator (9030 DS, Sciencetech) and a microchannel plate photomultiplier (R3809U, Hamamatsu). A time-correlated single photon counting PC module (SPC 630, Picoquant GmbH) was used to obtain fluorescence decay histograms in 4096 channels with time increments of 5 ps. In some cases additionally, a time increment of 0.8 ps was used in order to obtain reliable results for the shortest time components. Samples of the compound of interest dissolved in toluene with an absorption of ~0.1 per cm were measured under ambient conditions (temperature, pressure, atmosphere).

**Analysis.** For the femtosecond upconversion data, the 45 decay curves measured in all three time windows at detection wavelengths from 530 to 670 nm (low-wavelength region) were put together into a common data set which was analyzed

globally using a nonlinear least-squares fit routine from a commercial software package. As part of the analysis, the data sets were also deconvoluted using information from system prompt response measurements that were routinely recorded during each measurement session. After that, the data acquired in the high-wavelength range from 670 to 750 nm (9 wavelengths, 27 data sets) were treated identically, including the fit, using a global analysis. It turned out that the resulting partial amplitudes at the detection wavelength of 670 nm (which was included both in the high-wavelength and low-wavelength fits) were virtually identical for all components. As a consequence, the results as shown in the figures below appear as one line for each component which ranges from 530 nm to 750 detection wavelength.

The SPT data were analyzed globally with pulse deconvolution using a time-resolved fluorescence analysis program.[24] The quality of the fits was judged using the $\chi^2$ values ($<1.2$ for individual decays and globally $< 1.1$) and by visual inspection of the residuals and the autocorrelation function.

The numbering of the kinetic components 1...7 (times $\tau_1...\tau_7$) is used consistently throughout this paper, even if some of the components are not present in all samples.

## Results and Discussion

The analysis of the time-resolved data was performed in two different series for the fluorescencence upconversion data sets and for the SPT results. These two techniques are complementary in their corresponding time resolutions: for the former, the system prompt response was 250 fs, while the longest separable component time is ca. 1 ns (depending on the partial amplitude), as the maximum delay in the corresponding measurements was 450 ps. Any times exceeding this window will jointly be seen as a "long" component in the analysis and marked accordingly in the figures. Vice versa, the largest employed time window of the SPT setup is 20 ns so longer decay times can be studied, while system prompt response is ca. 30 ps. All times much below this cannot be separated even using global analysis and deconvolution procedures and hence appear jointly as one "short" component in the analysis and the figures. Only the time range of 100−500 ps is accessible and precisely resolved in both techniques. Upon combination of these two analysis approaches, for all samples all components in this region did match their respective counterpart in the other analysis, thus confirming all measurements and calculation and fit procedures.

For reference purposes, the fluorescence decay kinetics of separate donor and acceptor attached to the dendritic polyphenylene skeleton is needed. The results for the acceptor will be presented and discussed below. The fluorescence of the donor chromophore has previously been found to decay monoexponentially with a time constant of 4.0 ns.[24] Additionally, a vibrational/solvent relaxation process with a time constant of 4 ps has been determined by fluorescence upconversion measurements.[23] The corresponding absorption and emission spectra are shown in Figure 1A (marked P).

In all previous femtosecond fluorescence measurements on dendrimers decorated with chromophores,[15−17,28] a subpicosecond ultrafast component has been determined, which exhibits a time constant that is dependent on the detection wavelength and is attributed to an internal vibrational reorganization (IVR) process. A similar time constant is also seen with a low partial amplitude in most of the measurements reported here. It is likewise attributed to an IVR process and not discussed any further.

*1. Terrylenediimide Chromophore, T.* The steady-state absorption (left) and fluorescence spectra (right) of terrylenediimide dissolved in toluene are displayed in Figure 1A. They exhibit an absorption maximum at 651 nm along with a shoulder at 598 nm; the width of the main maximum is 590 $cm^{-1}$ (fwhm). This shape very closely resembles a miror image in the fluorescence spectrum (right part of the figure). Fluorescence is by far the most prominent pathway of deactivation for **T** as indicated by its fluorescence quantum yield of 0.99.

In the SPT measurements ($\lambda_{exc} = 590$ nm) of T, a monoexponential decay with a time constant of $\tau_6 = 3.2$ ns is measured. Upon global analysis of the femtosecond upconversion experiments ($\lambda_{exc} = 625$ nm), two kinetic components are found to be necessary to fit the data properly, as judged by the $\chi^2$ values and visual inspection of the residual plots. The results are shown in Figure 2 (amplitudes) and Table 1 (times). A small fast component with a time constant of $\tau_1 = 6.8$ ps is revealed, which shows a very similar time and a similar wavelength variation of the amplitudes (Figure 2, *) as known from previous experiments performed on peryleneimide[17] and is attributed to a vibrational and solvent relaxation process going on in the excited $S_1$ state of T immediately after excitation. The 3.2 ns component has by far the largest partial amplitude (>90% in upconversion, 100% in SPT) at all wavelengths between 660 and 750 nm (Figure 2, ●) and is straightforwardly attributed to the fluorescence decay of the terrylenediimide chromophore.

*2. Terrylenediimide with First Generation Dendritic Arms, T1P0.* The steady-state absorption and emission spectra of $T1P_0$ are shown in Figure 1B. As can be seen from the figure, both the absorption and emission spectra are red shifted by ca. 620 $cm^{-1}$ compared to the spectra obtained from the chromophore T alone. Moreover, a broadening of both the absorption and fluorescence spectrum is observed as compared to T, which is, for instance, seen in the main peak of the fluorescence spectrum which is increased to 750 $cm^{-1}$ (fwhm). The broadening can be rationalized by the fact that the additional sidearms of the molecule lead to a terrylenediimide ground state that is twisted, giving rise to a distribution of conformations (see Scheme 2).[31] With respect to T, the quantum yield of fluorescence of $T1P_0$ is only slightly reduced to 0.91. The additional band around 450 nm relates to a $S_0 \rightarrow S_2$ absorption which could be certified by SPT fluorescence anisotropy measurements indicating a limiting anisotropy of $-0.15$.[31]

The time-resolved decays recorded for $T1P_0$ cannot be fitted with two kinetic components any longer. Instead, in all cases a sum of four exponentials is necessary to fit the data properly. The results of the global analysis are shown in Figure 3, the times are collected in Table 1. The fastest time constant $\tau_1$ is found as 5.5 ps. This value and the wavelength dependence of the amplitudes (Figure 3A, *), which is very similar to the one observed for T, yield strong arguments to attribute this component to a vibrational/solvent relaxation process, which is going on in the excited state following the same line of argumentation as for T above.

The longest time constant $\tau_6$ for $T1P_0$ is determined as 3.2 ns (see Table 1), with amplitudes as shown in Figure 3A and B (●) Again, the partial amplitude of this component yields the largest contribution to the complete intensity. It increases from 50% at 670 nm to more than 80% at wavelengths longer than 700 nm. Comparing it to the decay time observed for T (see above), this time constant is attributed to fluorescence of the relaxed terrylenediimide chromophore.

A more detailed discussion is necessarry to explain time constant $\tau_5 = 900$ ps (see Table 1 and Figure 3B □). It is

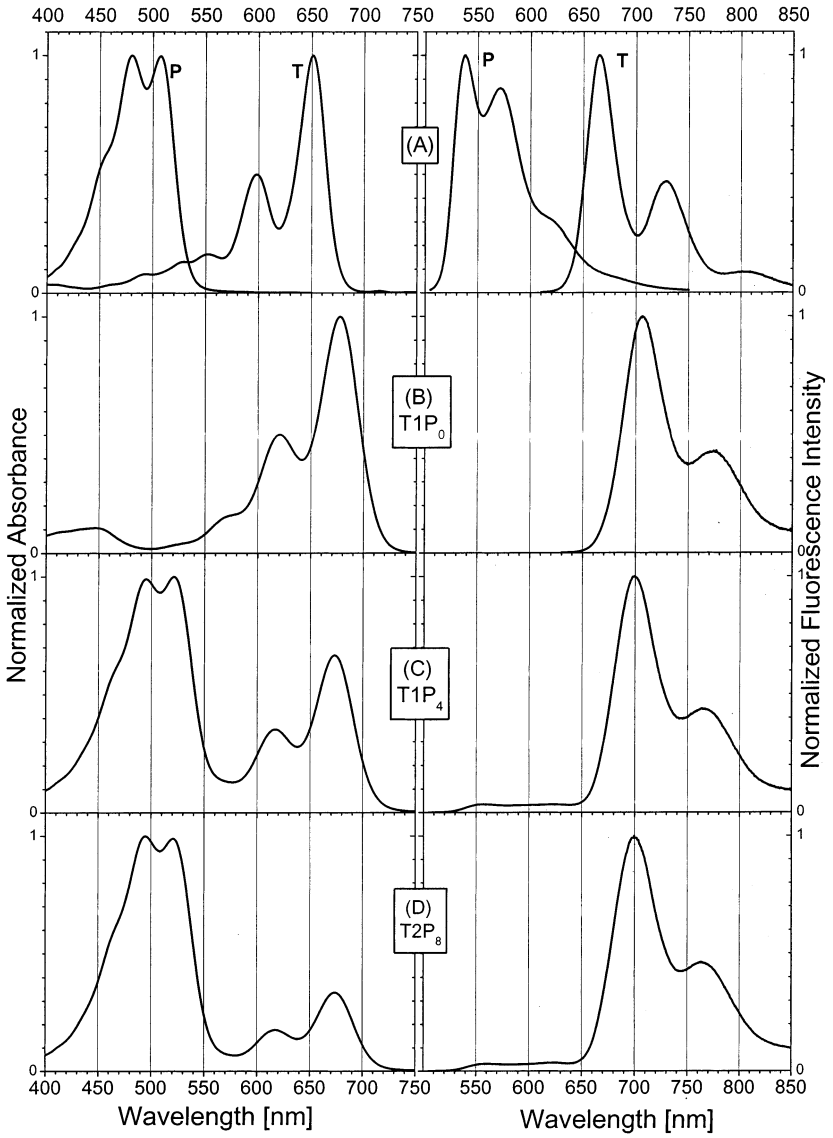


**Figure 1.** Steady-state absorption (left) and emission spectra (right) of (A) the bare terrylenediimide chromophore T and peryleneimide P; (B) the first generation model compound ($T1P_0$); (C) the first generation donor−acceptor dendrimer $T1P_4$; and (D) the second generation donor−acceptor dendrimer $T2P_8$. Emission spectra were taken using excitation at 495 nm.

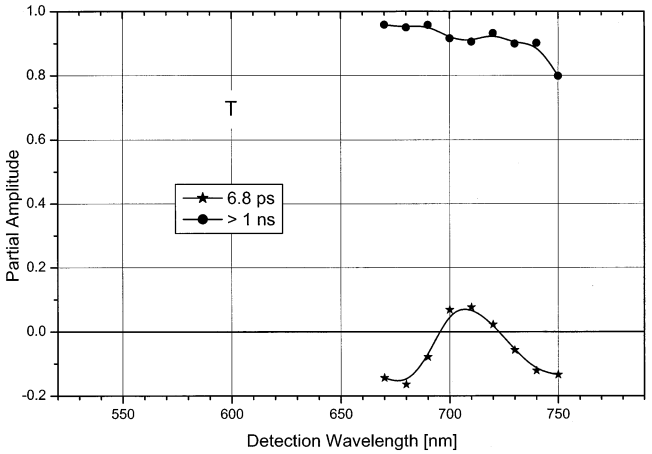


**Figure 2.** Wavelength dependencies of the partial amplitudes of the kinetic components resulting from a global analysis of the data acquired for the chromophore model compound T. Excitation was done at a wavelength of 625 nm.

positive between 670 and 700 nm, crossing zero at 700 nm, and is negative between 700 and 780 nm. This behavior is indicative of a transition between two states as shown schematically by B and $S_1$ in Figure 4B. At wavelengths lower than 700 nm it is seen as a decaying emission from the state B, while above 700 nm the same process is seen from the state $S_1$ as a rise term. The overall partial amplitude of this process, however, is 10% at the maximum and at most wavelengths even lower. Is important to note that this component decreases in amplitude at wavelengths between 660 and 710 nm (Figure 3B, □), while the amplitudes of the terrylenediimide fluorescence component $\tau_6$ increase correspondingly in the same wavelength range (Figure 3B, ●). This can be rationalized only by the assumption that the former is an independent precusor for the 3.2 ns fluorescence process as shown in the term scheme in Figure 4B. However, not all molecules in the sample show this behavior; for the majority this precursor is not observed. For this main group a very fast relaxation process A → $S_1$ of 5.5 ps (see Figure 4A) is observed, which is attributed to vibrational/solvent relaxation. The molecules that are members of a second independent subgroup undergo the transition B → $S_1$ with a time constant of 900 ps. One possibility would be the occurrence of aggregation; however, the fact that data from upconversion and SPT measurements fully overlap although there is a 40-

**TABLE 1: Summary of the Time Constants Found for All Kinetic Components Discussed in the Text[a]**

| | | | T | | $T1P_0$ | | $T1P_4$ | | $T2P_8$ | |
|---|---|---|---|---|---|---|---|---|---|---|
| | symbol | attribution | UC | SPT | UC | SPT | UC | SPT | UC | SPT |
| 1 | * | vib./solvent relaxation | 6.8 | *b* | 5.5 | *b* | 4 | } 15 | 6 | } 27 |
| 2 | ▲ | energy transfer | *b* | *b* | *b* | *b* | 4 | | 22 | |
| 3 | △ | energy transfer | *b* | *b* | *b* | *b* | 22 | | 68 | } 92 |
| 4 | ■ | structural relaxation | *b* | *b* | 120 | 115 | 200 | 240 | *b* | |
| 5 | □ | structural relaxation | *b* | *b* | } > 1000 | 900 | } > 1000 | 1300 | } > 1000 | 1000 |
| 6 | ● | terrylenediimide fluor. | > 1000 | 3200 | | 3200 | | 3200 | | 3200 |
| 7 | ○ | peryleneimide fluor. | *b* | *b* | *b* | *b* | | 4000 | | 4000 |

[a] All values are times in ps. [b] Experimentally not found. UC = upconversion; SPT = single photon timing.

**SCHEME 2: Structures of the Terrylenediimide Core of $T1P_0$ for Different Relative Orientations of the Dendritic Arms[a]**

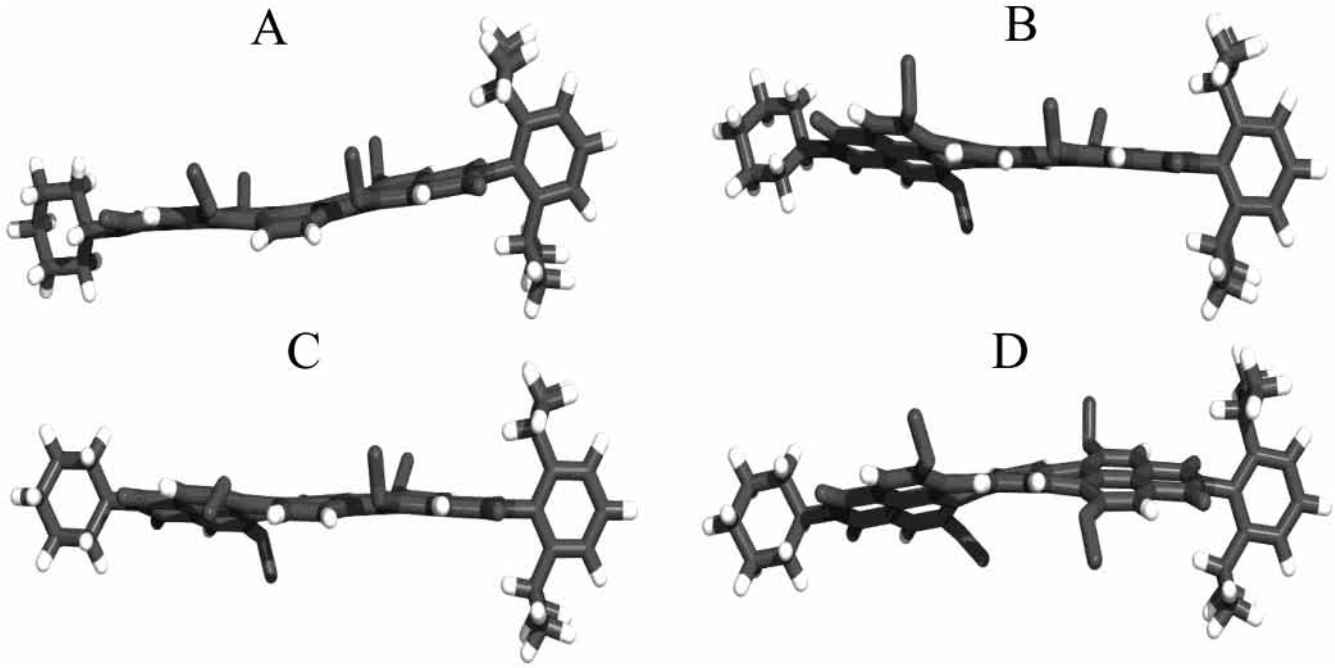


[a] The arms are omitted for clarity. (A) All four arms above the plane of the terrylene; (B) three arms above and one arm under the plane; (C) two arms above and two arms under in pairs; and (D) alternatingly two arms above and two arms under.

fold concentration difference makes this unlikely. This subgroup is possibly related to a structural isomer in which the dendritic arms attached to the central terrylenediimide impose a twist into the central terrylenediimide moiety (vide infra, see Scheme 2). The 900 ps time constant kinetic component 5 thus relates to structural relaxation within the terrylenediimide (which is hindered in this way).

The fourth and final kinetic component is determined with a time constant of $\tau_4 = 115$ ps (see Table 1) and amplitudes as shown in Figure 3 (■). The general tendency of these partial amplitudes quite closely resembles the results reported above for the 900 ps component. Thus, following the same line of argumentation, this component is also attributed to a structural relaxation process within the terrylenediimide, which is going on in yet another subgroup of all molecules ($C \rightarrow S_1$ in Figure 4C). In this third subgroup, the structural relaxation process is also slower than the one in the majority part; however, not as slow as the one described above.

In line with this interpretation it is found from molecular modeling that the presence of the dendritic arms imposes a distortion of the terrylenediimide chromophore. Whereas the bare T chromophore is flat, the aromatic skeleton is bent out-of-plane in $T1P_0$. Moreover, the different relative orientations of the dendritic arms seem to impose different distortions of the terrylene skeleton. It was found that the distortions are not influenced by the nature of the arms (different generations) but only by their relative orientation. Four different situations can be envisaged: all arms above the plane of the terrylene (Scheme 2A), three above and one under (Scheme 2B), two above and two under in pairs (Scheme 2C), or alternating (Scheme 2D). We attribute the 115 and 900 ps time constants to decay channels that reflect the presence of various conformations of the terrylene skeleton that finally end up in a common emitting state for all conformers. Since the conformation of the aromatic system is governed only by the relative orientation of the substituents and not by their nature, the same components are also expected for the donor−acceptor dendrimers.

*3. Second Generation Dendrimes, $T2P_8$.* The absorption spectra (left), which are the composition of the respective model compounds, and the fluorescence emission spectra (right) of $T2P_8$ are shown in Figure 1D; the latter was recorded using an excitation wavelength of 495 nm which is close to the absorption maximum of the peryleneimide chromophore. Upon comparison to the peryleneimide spectra shown in Figure 1A, a very strong quenching of the peryleneimide fluorescence is seen. At wavelengths longer than 650 nm, the fluorescence of $T2P_8$ almost completely resembles the emission spectrum of the model compound $T1P_0$. This behavior alone is already a strong indication for the fact that in the donor−acceptor system peryleneimide−terrylenediimide the optical excitation into the

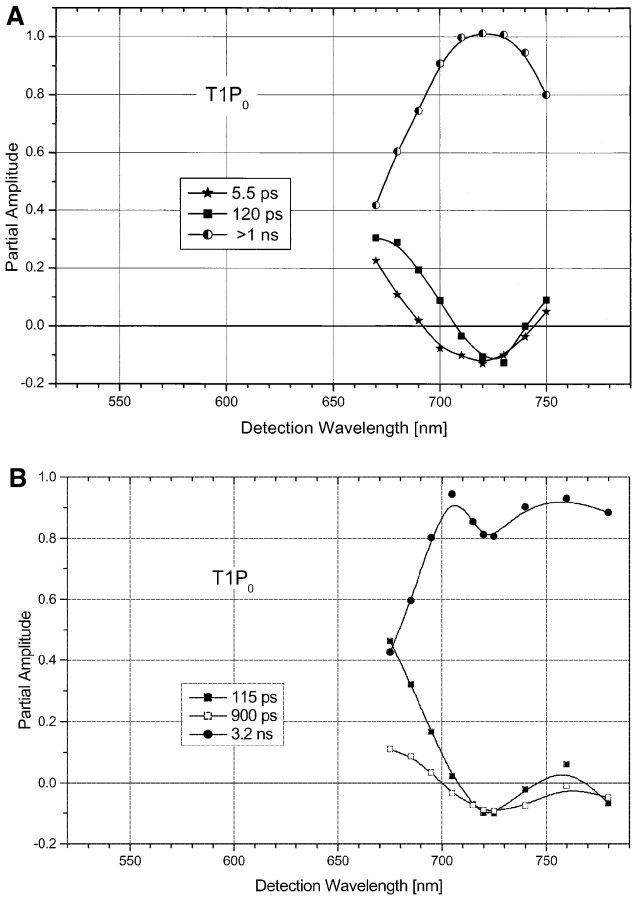


**Figure 3.** Wavelength dependencies of the partial amplitudes of the kinetic components resulting from a global analysis of the data acquired for the model compound $T1P_0$. (A) Upconversion results, (B) SPT results. Excitation was done at a wavelength of 625 nm (upconversion) and 590 nm (SPT).

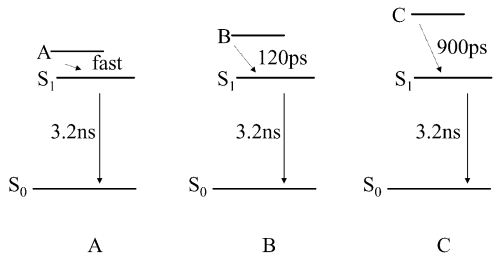


**Figure 4.** Proposed kinetic model of various processes going on in terrylenediimide immediately after excitation. (A) majority subgroup; (B) and (C) minority subgroups. In all cases, vibrational/solvent relaxation is assumed to be finished.

peryleneimide is very efficiently transferred into the terrylenediimide chromophore.

In the analysis of the time-resolved data sets acquired both from femtosecond upconversion measurements and SPC detection, a total of seven kinetic components could be determined. The corresponding amplitudes are shown in Figure 5A (shorter times, femtosecond results) and Figure 5B (longer times, SPC results). All resulting times are collected in Table 1.

As expected, all the kinetic components found and attributed to the reference compound $T1P_0$ were found again for this sample with very minor changes. Thus, component 1 ($\tau_1 = 6$ ps, * in Figure 5A) is attributed to a vibrational/solvent relaxation process. This component might also contain a minor contribution from a possible singlet−singlet annihilation process

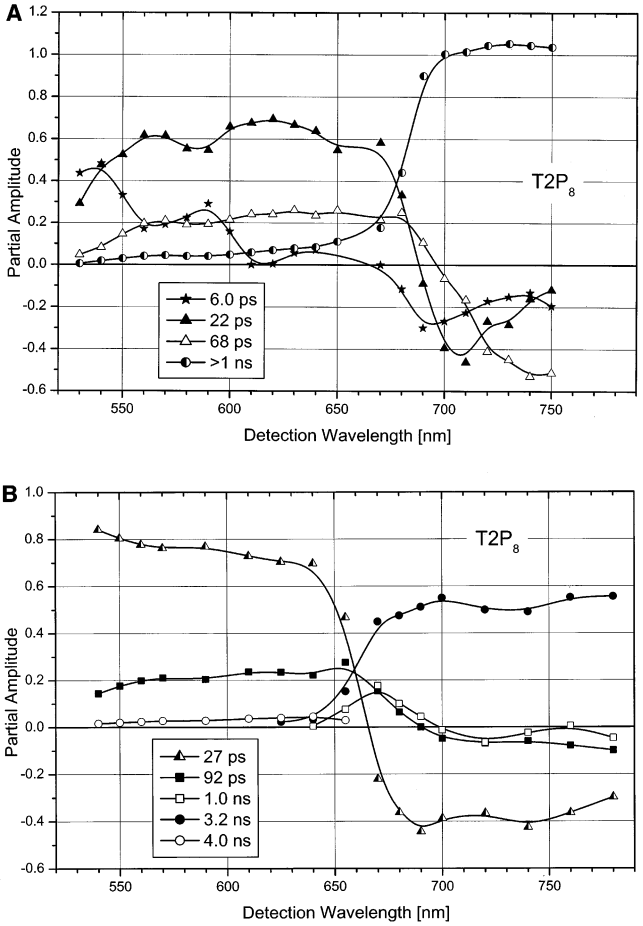


**Figure 5.** Wavelength dependencies of the partial amplitudes of the kinetic components resulting from a global analysis of the data acquired for the second generation dendrimer $T2P_8$. (A) Upconversion results, (B) SPT results. Excitation was done at a wavelength of 495 nm.

having a very similar time constant. The component 5 is assigned to structural relaxation of the terrylenediimide chromophore ($\tau_5 = 1.0$ ns, □ in Figure 5B), component 6 ($\tau_6 = 3.2$ ns, ● in Figure 5A and B) is again attributed to the terrylenediimide fluorescence.

The major difference compared to the results of the model compound $T1P_0$ is the finding of two additional kinetic components 2 and 3. The first one of these is determined with a time constant of $\tau_2 = 22$ ps for upconversion and 27 ps for SPC, which is within experimental error. The corresponding wavelength dependence of the amplitude $a_2$ is also displayed in Figure 5A (▲). It exhibits a maximum around 610 nm being positive up to a wavelength of 685 nm, i.e., throughout the complete fluorescence region of the peryleneimide. At wavelengths longer than this, i.e., in the emission region of the terrylenediimide, this component becomes negative with one maximum at ca. 710 nm. The amplitudes from the SPC measurements display a similar general trend (Figure 5B). A behavior like this is a very strong indication of an energy transfer process with the determined time constant of 22 ps. This process starts in the excited state of the peryleneimide (donor) and ends in the excited state of the terrylenediimide (acceptor).

The second of the additional kinetic components is determined with a time constant of $\tau_3 = 68$ and 92 ps for upconversion and SPT, respectively. The value of the SPT measurements may be slightly higher because it is actually a convolution of $\tau_3$ and $\tau_4$, which cannot be resolved due to the similar spectrum and the overall low amplitude of the latter (vide infra). The

corresonding amplitude distribution of $a_3$ is also shown in Figure 5A (upconversion, △) and Figure 5B (SPC, △). Again, a positive maximum in the fluorescence region of the peryleneimide donor is determined. Upon increasing wavelength, the amplitude crosses zero at 695 nm, showing one single negative maximum in the fluorescence region of the terrylenediimide acceptor. Thus, the overall shape is very similar to the one described above for component 2. With the same argumentation, this component 3 is attributed to a second independent energy transfer process going on in the perylene−terrylene donor−acceptor system. The finding of two different energy transfer processes could be rationalized by the assumption of two different isomeric subgroups of molecules which differ in their relative donor−acceptor orientations and/or distances. One main difference is the smaller overall amplitude of this second component, which corresponds to a relatively smaller probability of the system following the underlying energy transfer pathway or reflects the lower relative contribution of the corresponding structural isomer. If we examine the partial amplitudes of all kinetic components in the wavelength range of the acceptor emission, it can be seen that the ratio of all negative to all positive amplitudes is close to −1. For instance, at 740 nm this value is −1.04 in the case of the SPT measurements. This indicates that all emission at these wavelengths are accounted for by the rise components at these wavelengths, i.e., the energy transfer components.

The structural relaxation component ($\tau_4$, $a_4$) which had been found in $T1P_0$ is not isolated in the analysis here, which is most probably due its very low overall amplitude and the close proximity of the time constant (115 ps) to the above-mentioned energy transfer component (92 ps).

Finally, another component with a time constant $\tau_7 = 4.1$ ns and an overall small amplitude is seen in upconversion (Figure 5A, ○) and determined in SPC analysis results (Figure 5B, ○). The identical time constant together with the fact that the corresponding amplitudes are only nonzero in the peryleneimide emission region give a strong argument to assign this component to a peryleneimide fluorescence emission, which has been reported previously.[24] However, this emission cannot be attributed to energy transferring peryleneimides, as the energy transfer quantum yield is much too high to allow for a competing partial amplitude of ca. 5% and the decay time is virtually unchanged with respect to the donor in the absence of acceptor. Instead, this component is attributed to a number of molecules in which the peryleneimide is either functionally decoupled or the terrylendiimide is not fully ring closed and thus cannot take part in the energy transfer process. This assignment is supported by observations in single molecule experiments, where occasionally molecules are seen that only give peryleneimide fluorescence emission, but never molecules that give partial energy transfer.[11]

*4. First Generation Dendrimers, T1P4.* In a further series of experiments, the first generation dendrimer $T1P_4$ was measured and analyzed in a manner identical to that reported for $T2P_8$. The steady-state absorption and emission spectra (see Figure 1C) are very similar to those of the second generation dendrimer $T2P_8$. The only difference is the relative intensity of the terrylenediimide band as compared to the perylenediimide, which is a direct consequence of the halved (4:1 versus 8:1) relative amount of peryleneimide chromophores per molecule. In the global analysis for the data acquired from this compound, a sum of six exponentials was needed to get a satisfactory fit, the results are shown in Figure 6A (upconversion results), Figure 6B (SPC results), and Table 1.

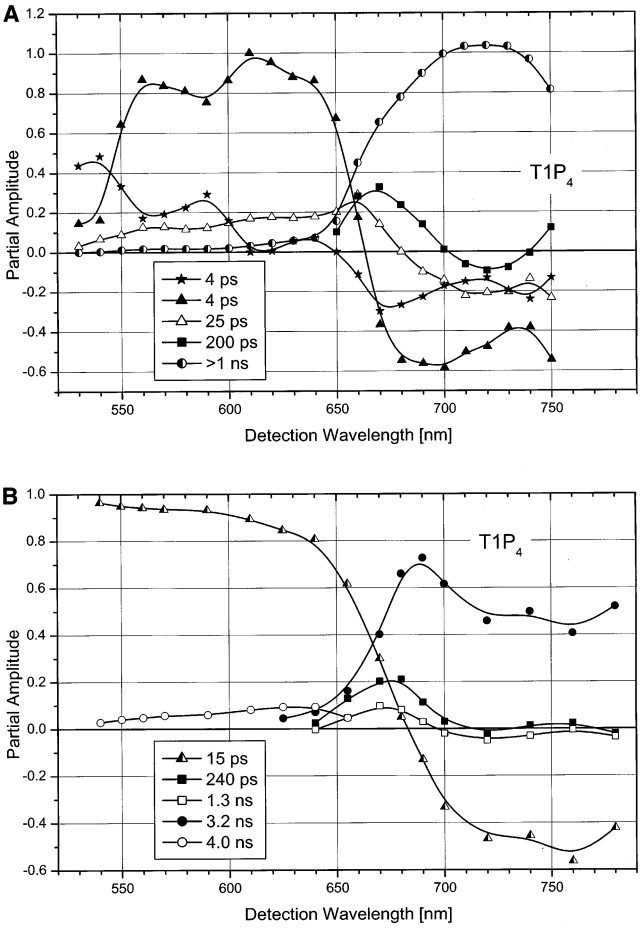


**Figure 6.** Wavelength dependencies of the partial amplitudes of the kinetic components resulting from a global analysis of the data acquired for the first generation dendrimer $T1P_4$. (A) Upconversion results, (B) SPT results. Excitation was done at a wavelength of 495 nm.

The fastest kinetic component is determined as $\tau = 4$ ps. However, the related partial amplitude exhibits a shape and wavelength dependence which is in no way similar to any of the results found before both for peryleneimide- and terrylenediimide-containing samples. Given the results from previous studies,[16,17,23] which show that the vibrational/solvent relaxation component is always present, it is reasonable to assume that it is present here as well and making up for one part of the 4 ps component. Thus, this component in fact stems from the superposition of two different and competitive kinetic processes which cannot be resolved by the global analysis because their time constants are very close to each other and ca. 4 ps in both cases (see Figure 4). To split these, it is assumed that the vibrational/solvent relaxation component is very similar to the kinetics found in $T2P_8$, so this can be considered as the first contribution ($\tau_1$, $a_1$) to the 4 ps component (Figure 6A, *). As the spectral shift related to this process is less than 5 nm (vide supra), it does not have a large effect upon overlap integrals and processes governed by the Förster mechanism.

The remaining amplitude is attributed to a second competitive component 2 ($\tau_2 = 4$ ps) and shown in Figure 6A as ▲ line, which resembles the general shape of the energy transfer component 2 as found in $T2P_8$. With this observation and the same arguments as mentioned above for $T2P_8$, this component is attributed to an energy transfer process from the peryleneimide to the terrylenediimide chromophore.

The third component ($\tau_3$, $a_3$) is determined with a time constant of $\tau_3 = 25$ ps and a wavelength dependence as shown

in Figure 6A (△). This wavelength dependence and the general shape are very similar to the ones found for component 3 in the second generation dendrimers $T2P_8$. Again, the finding of *two* energy transfer processes could be rationalized by the assumption of two different subgroups of molecules which differ in their isomeric state. The relative ratios of the negative and positive partial amplitudes once more indicate that the fluorescence in the wavelength range of the acceptor emission (>700 nm) entirely stems from the rise components and thus is formed via initial energy transfer.

In addition, all longer time components determined for the model compound $T1P_0$ are again found back here. The components 4 and 5 (Figure 6B, ■ and □, respectively) are determined with time constants $\tau_4 = 200$ and 240 ps (for upconversion and SPT, respectively) and $\tau_5 = 1.3$ ns. With an identical argumentation as discussed above for the reference compound $T1P_0$, they are both attributed to structural relaxation processes going on in the terrylenediimide chromophore. The suggestion that $\tau_5$ reflects a process that is only going on in the terrylenediimide chromophore is corroborated by the finding that it only has a significant amplitude at emission wavelengths higher than 650 nm.

This is, however, not the case for $\tau_4$. No satisfactory fits could be obtained when the contribution of this component was set to zero in the wavelength regime below 650 nm. Good fits were obtained when this parameter was set free, although its partial amplitude remained quite low.

Also in this compound a fluorescence component 6 ($\tau_6 = 3.2$ ns, amplitudes ● in Figure 6B) is determined and assigned to terrylenediimide fluorescence emission.

Finally, a residual 4.0 ns fluorescence is found (Figure 6B, ○) at wavelengths shorter than 630 nm with a small partial amplitude over its entire range, which stems from uncoupled peryleneimide chromophores in the same way as attributed to $T2P_8$ above.

**Förster Energy Transfer.** The finding of an energy transfer process as described above is consistent with the strong fluorescence quenching seen in the steady-state spectroscopy of these dendritic systems (Figure 1C and D), both containing peryleneimide chromophores at the rim and a terrylenediimide chromophore in the core. Within the framework of the Förster formulation an effective interaction radius $R_0$ can be calculated from the steady-state spectra and the fluorescence quantum yield (ref 23 and references therein) of the donor chromophore ($\phi_D$) as 5.9 nm, assuming $\kappa^2 = 2/3$. The donor−acceptor center-to-center distances within the dendrimers depend on the conformation of the dendritic arm. From molecular modeling, representative values of 2.3 nm for $T1P_4$ and 3.1 nm for $T2P_8$ are obtained, which are well within the Förster radius, giving another strong argument for the presence of an efficient energy transfer process. From these donor−acceptor distances combined with the Förster distance $R_0$, deacy times of energy transfer of 14 and 84 ps are calculated for the first and second generation, respectively. These times correspond well with the experimentally obtained decay times, bearing in mind the asumption of $\kappa^2$ and that there will be a distribution of donor−acceptor distances and orientations.

For both generations of the donor−acceptor dendrimers, two energy transfer components were obtained. The fact that the two time constants are shorter compared to the ones determined for the second generation dendrimer $T2P_8$ is explained by the decreased average distance between donor and acceptor site. Assuming a Förster type process, a ratio of $D_2$:$D_1 = 3.1$ nm: 2.3 nm = 1.3 in the distances would yield an increase in the transfer time of a factor of $(1.3)^6 = 6$, which is almost exactly what is found for the fast energy transfer component (25 ps: 4 ps = 6.3). Comparing the femtosecond upconversion time constants of the slower energy transfer component (68 ps: 25 ps = 2.7), a somewhat smaller difference between first and second generation is found. One possible explanation could lie in the competition energy hopping between identical chromophores within one arm.[23] Considering that the two donor−acceptor distances in the dendrimers are only average distances and that the orientation factor $\kappa^2$ is assumed to be equal for both generations, this difference seems reasonable.

## Conclusions

The time-resolved fluorescence properties of first and second generation dendrimers containing peryleneimide chromophores at the rim and a terrylenediimide chromophore in the core have been investigated using femtosecond fluorescence upconversion and single photon timing techniques. By globally analyzing data sets from upconversion and SPT measurements and comparing the results both to previous results from peryleneimide-only dendrimers and a terrylenediimide reference compound, we were able to find, identify, and attribute various kinetic components.

Much like in the dendrimers containing only one type of chromophore(s), the vibrational/solvent relaxation in the excited state (4 ps...6.8 ps, depending on the compound) could be attributed. Also, the fluorescence of the chromophore (3.2 ns in terrylenediimide) was seen at a relatively large partial amplitude.

Most importantly, however, two new kinetic components could be determined both in the first and second generation dendrimers, which were seen neither in the previous results from peryleneimide-only dendrimers[16,17,23] nor upon direct excitation into the terrylenediimide absorption bands. This pair of times is found in the first generation (4 ps, 25 ps) as well as in the second generation (22 ps, 68 ps). Both times are attributed to two independent different energy transfer process occurring between the perylenimide donor and the terrylenediimide acceptor system. The shorter and longer times, respectively, can be attributed to transfers going on in two different structural isomers of the dendritic molecules. This attribution is−among other arguments−supported by the fact that the fastest times in the pairs scale with the sixth root of the ratio of distances in first and second generation.

Two additonal kinetic components with time constans of ca. 150 ps and ca. 1.2 ns are attributed to structural relaxation processes going on in the terrylenediimide chromophore of a fraction of the molecules before the fluorescing state is reached.

**Acknowledgment.** The authors gratefully acknowledge the FWO, the Flemish Ministry of Education for the support through GOA 1/96, the EC through the TMR Sisitomas, the Bundesministerium for Education and Research of the Federal Republic of Germany, the Volkswagenstiftung and the support of DWTC (Belgium) through IUAP-V-03. Financial contribution through the research price of the Max-Planck-Gesellschaft is gratefully acknowledged.

## References and Notes

(1) Gopidas, K. R.; Leheny, A. R.; Caminati, G.; Turro, N. J.; Tomalia, D. A. *J. Am. Chem. Soc.* **1991**, *113*, 7335.

(2) Hawker, C. J.; Frechet, J. M. In *Step-Growth Polymers for High-Performance Materials*; Hedrick, J. L., Labadie, J. W., Eds.; Oxford University Press: Oxford, 1996.

(3) Aoi, K.; Itoh, K.; Okada, M. *Macromolecules* **1995**, *28*, 5391.

(4) Archut, A.; Vogtle, F. *Chem. Soc. Rev.* **1998**, *27*, 233.

(5) Zimmermann, S. C.; Zeng, F. W.; Reichert, D. E. C.; Kolotuchin, S. V. *Science* **1996**, *271*, 1095.

(6) Frechet, J. M. *Science* **1994**, *263*, 1710.

(7) Tomalia, D. A. *Top. Curr. Chem.* **1993**, *165*, 193.

(8) Morgenroth, F.; Kubel, C.; Müllen, K. *J. Mater. Chem.* **1997**, *7*, 1207.

(9) Vosch, T.; Hofkens, J.; Cotlet, M.; Köhn, F.; Fujiwara, H.; Gronheid, R.; Van der Biest, K.; Weil, T.; Herrmann, A.; Müllen, K.; Mukamel, S.; Van der Auweraer, M.; De Schryver, F. C. *Angew. Chem., Int. Ed.* **2001**, *40*, 4643.

(10) Hofkens, J.; Maus, M.; Gensch, T.; Vosch, T.; Cotlet, M.; Köhn, F.; Herrmann, A.; Müllen, K.; De Schryver, F. C. *J. Am. Chem. Soc.* **2000**, *122*, 9278.

(11) Gronheid, R.; Hofkens, J.; Köhn, F.; Weil, T.; Reuther, E.; Müllen, K.; De Schryver, F. C. *J. Am. Chem. Soc.* **2002**, *124*, 2418.

(12) Vosch, T. Doctoral Thesis, in preparation.

(13) Hofkens, J.; Verheijen, W.; Shukla, R.; Dehaen, W.; De Schryver, F. C. *Macromolecules* **1998**, *31*, 4493.

(14) Gensch, T.; Hofkens, J.; Heirmann, A.; Tsuda, K.; Verheijen, W.; Vosch, T.; Christ, T.; Basche, T.; Müllen, K.; De Schryver, F. C. *Angew. Chem., Int. Ed.* **1999**, *38*, 3752.

(15) Karni, Y.; Jordens, S.; De Belder, G.; Hofkens, J.; Schweitzer, G.; De Schryver, F. C.; Herrmann, A.; Müllen, K. *J. Phys. Chem. B* **1999**, *103*, 9378.

(16) De Belder, G.; Jordens, S.; Lor, M.; Schweitzer, G.; De, R.; Weil, T.; Herrmann, A.; Wiesler, U. K.; Müllen, K.; De Schryver, F. C. *J. Photochem. Photobiol.* **2001**, *145*, 61.

(17) De Belder, G.; Schweitzer, G.; Jordens, S.; Lor, M.; Mitra, S.; Hofkens, J.; De Feyter, S.; Van der Auweraer, M.; Herrmann, A.; Weil, T.; Müllen, K.; De Schryver, F. C. *Chem. Phys. Chem.* **2001**, *2*, 49.

(18) Gensch, T.; Hofkens, J.; Van Stam, J.; Faes, H.; Creutz, S.; Tsuda, K.; Jerome, R.; Masuhara, H.; De Schryver, F. C. *J. Phys. Chem. B* **1998**, *102*, 8440.

(19) Hofkens, J.; Schroeyers, W.; Loos, D.; Cotlet, M.; Köhn, F.; Vosch, T.; Maus, M.; Herrmann, A.; Müllen, K.; Gensch, T.; De Schryver, F. C. *Spectrochim. Acta A* **2001**, *57*, 2093.

(20) Morgenroth, F.; Reuther, E.; Müllen, K. *Angew. Chem., Int. Ed.* **1997**, *36*, 631.

(21) Morgenroth, F.; Müllen, K. *Tetrahedron* **1997**, *53*, 15349.

(22) Morgenroth, F.; Kubel, C.; Muller, M.; Wiesler, U. M.; Berresheim, A. J.; Wagner, M.; Müllen, K. *Carbon* **1998**, *36*, 833.

(23) Lor, M.; De, R.; Jordens, S.; De Belder, G.; Schweitzer, G.; Cotlet, M.; Hofkens, J.; Weil, T.; Herrmann, A.; Müllen, K.; Van der Auweraer, M.; De Schryver, F. C. *J. Phys. Chem. A* **2002**, *106*, 2083.

(24) Maus, M.; De, R.; Lor, M.; Weil, T.; Mitra, S.; Wiesler, U. M.; Herrmann, A.; Hofkens, J.; Vosch, T.; Müllen, K.; De Schryver, F. C. *J. Am. Chem. Soc.* **2001**, *123*, 7668.

(25) Weil, T.; Reuther, E.; Müllen, K. *Angew. Chem., Int. Ed.* **2002**, *41*, 1900.

(26) *Principles of Fluorescence Spectroscopy*; Lakowicz, J. R., Ed., Plenum: New York, 1999; p 53.

(27) Schweitzer, G.; Xu, L.; Craig, B.; De Schryver, F. C. *Opt. Commun.* **1997**, *142*, 283.

(28) Karni, Y.; Jordens, S.; De Belder, G.; Schweitzer, G.; Hofkens, J.; Gensch, T.; Maus, M.; De Schryver, F. C.; Hermann, A.; Müllen, K. *Chem. Phys. Lett.* **1999**, *310*, 73.

(29) Hofkens, J.; Latterini, L.; De Belder, G.; Gensch, T.; Maus, M.; Vosch, T.; Karni, Y.; Schweitzer, G.; De Schryver, F. C.; Hermann, A.; Müllen, K. *Chem. Phys. Lett.* **1999**, *304*, 1.

(30) Maus, M.; Rousseau, E.; Cotlet, M.; Schweitzer, G.; Hofkens, J.; Van der Auweraer, M.; De Schryver, F. C.; Krueger, A. *Rev. Sci. Instrum.* **2001**, *72*, 36.

(31) Hofkens, J.; Vosch, T.; Maus, M.; Köhn, F.; Cotlet, M.; Weil, T.; Herrmann, A.; Müllen, K.; De Schryver, F. C. *Chem. Phys. Lett.* **2001**, *333*, 255.